# Modified Michaelis law in a two-state ratchet model for a molecular motor as a function of diffusion constant

Hye Young Moon and Youngah Park
*Department of Physics, Myongji University, Yongin 449-728, Korea*
(Received 27 November 2002; published 21 May 2003)

We study transport properties and energetics of ratchets, which are driven by a chemical reaction between two states with different diffusion constants. We find that velocity curves show very sensitive dependence on the ratio of diffusion constants, whereas the rate of Adenosinetriphosphate (ATP) consumption curves depends smoothly on it. Modified Michaelis-Menten law shows us that identical values of Michaelis-Menten constant $K_M$ can be obtained independently from both curves. We obtain force-velocity curves for different values of a ratio of diffusion constants. We find that the Michaelis-Menten constant increases with the increasing external load for the ''active site'' model where the ATP assisted transition occurs at the localized region near the minimum of the ratchet potential, whereas it decreases with the increasing load for the ''delocalized model.''

DOI: 10.1103/PhysRevE.67.051918 PACS number(s): 87.16.Ac, 87.16.Nn, 05.40.−a

## I. INTRODUCTION

One of the essential features of biological systems is that they can transduce chemical energy into mechanical motion and work on a molecule scale. Important examples are muscle contraction, transport of materials and vesicles, cell mobility, and cell mitosis. Recent studies have shown that these motions and forces are generated on a molecular level by motor proteins that are driven by chemical reactions consuming ATP (Adenosinetriphosphate) in a far from equilibrium situation.

Linear motor proteins move along complex periodic structures called filaments, which are obtained by the polymerization of identical monomers (actin filaments) or dimers (microtubules). An important feature is their polarity, which originates from the asymmetry of monomers forming a polar structure with two different ends denoted by ''plus end'' and ''minus end.'' So far three different families of motor proteins have been identified: kinesins moving along microtubules are responsible for transport of organelles, myosins moving along actin filaments are responsible for muscle contraction, and dyneins are involved in cellular locomotion. Kinesins and myosins move toward the plus end, whereas dyneins move toward the minus end [1,2].

Several models have been studied to explain how the chemical energy of ATP is transduced into unidirectional motion of motor proteins [2–9]. A thermal ratchet models is one of the extensively studied models explaining the motion of motor proteins [4,5,10]. In a thermal ratchet model a motor protein diffuses as a Brownian particle in a several periodic, ratchetlike potential that is alternatively switched on and off in a stochastic way.

The role of the external load in the kinetics of motor proteins is of interest [11,12]. With the development of an optical force clamp, it became possible to observe precisely the motion of single motors along filaments while maintaining the constant load on them. An analysis of records of kinesin motion under variable ATP concentrations and loads indicates that the kinetics of ATP hydrolysis can be described by the Michaelis-Menten mechanism,

$$v = \frac{v_{\max}[\mathrm{ATP}]}{K_M + [\mathrm{ATP}]}. \tag{1}$$

Here [ATP] is the concentration of ATP, $v_{\max}$ is the velocity at saturating ATP, and $K_M$ is mechanochemical Michaelis-Menten constant [12]. However recent experiment on a single kinesin motor revealed some puzzling results: Increased loads reduce the maximum velocity as expected, but raise the apparent Michaelis-Menten constant by a factor of 4 when the external load increases five times [13]. Lattanzi and Maritan provide a modified Michaelis-Menten law to explain the puzzling data within the framework of coarse grained two-state ratchet models [14].

In this paper, we generalize a model introduced by Lattanzi and Maritan and study force-velocity relations in a general two-state ratchet model in which diffusion constants in each of the two states are different. By obtaining the Michaelis-Menten curve for various values of the ratios of diffusion constants, we find that an increase in Michaelis constant for increased loads is a property of the two-state ratchet model where ATP-hydrolysis transition occurs only in an ''active site'' and explain the obtained data using the modified Michaelis-Menten law. We find that in the model where the transitions are ''delocalized,'' the Michaelis-Menten constant decreases with increasing load. In Sec. II, the two-state ratchet model will be introduced. Simulation results will be provided in Sec. III. We discuss our result in the final section.

## II. TWO-STATE RATCHET MODEL

We now describe a two-state ratchet model for force generation and motion of a liner motor [5], in which ATP consumption triggers a conformational change between states 1 and 2. The free energy of the motor at state $i$ with the center of mass at position $x$ is described by the periodic and asymmetric potential $W_i(x)$. Introducing the probability density $P_i(x,t)$ for the motor to be at position $x$ at time $t$ in state $i$, the Fokker-Planck equations describing the evolution of the systems are

 

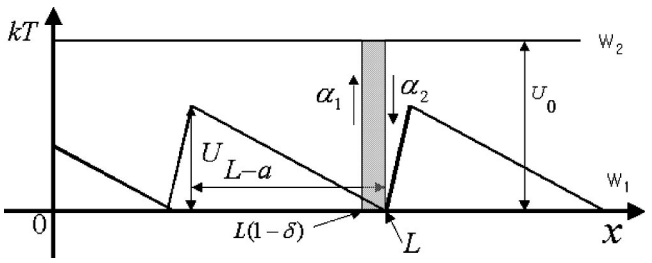


FIG. 1. A ratchet potential $W_1$ and diffusive state potential $W_2$. The parameters are set to $a/L=0.1$, the maximum of $W_1=10k_BT$, $W_2=12k_BT$. $\delta=0.05$ in model (a), $\delta=0.3$ in model (b), and $\delta=1$ in model (c).

$$\partial_t P_1+\partial_x J_1=-\omega_1(x)P_1+\omega_2(x)P_2, \tag{2}$$

$$\partial_t P_2+\partial_x J_2=+\omega_1(x)P_1-\omega_2(x)P_2, \tag{3}$$

where $\omega_1[\omega_2(x)]$ is the transition rate from the state 1 (state 2) to state 2 (state 1). The current density resulting from diffusion, interaction with the microtubule, and an external load $F_{\text{ext}}$ are given by

$$J_i=\frac{D_i}{k_BT}[P_i(x,t)\partial_x W_i-P_i(x,t)F_{\text{ext}}+k_BT\partial_x P_i(x,t)], \tag{4}$$

where $D_i$ is a diffusion constant in each state $i=1,2$. In a two-state model, the chemical reaction cycle can be described by introducing the forward and backward rates $\alpha_1$ and $\alpha_2$ for the combined process of ATP binding and hydrolysis

$$M+\text{ATP}\underset{\alpha_1}{\overset{\alpha_1}{\rightleftharpoons}}M\text{-ADP-}P, \tag{5}$$

and the rates $\beta_1$ and $\beta_2$ describing the process of product release and binding:

$$M+\text{ADP}+P\underset{\alpha_1}{\overset{\alpha_1}{\rightleftharpoons}}M\text{-ADP-}P, \tag{6}$$

where $M$ refers to the motor protein. The subsequent transitions $\alpha_1$ and $\beta_2$ complete the chemical reaction cycle. The state $M$-ADP-$P$ will be called the ''free' state,'' or state 2 corresponding to that in which the motor head is detached from the microtubule after binding and dissociating ATP. All other states in the reaction cycle will be called 'bound' state or state 1, corresponding to that in which the motor is attached to the microtubule.

We suppose that state 2 is strictly diffusive so that potential $W_2(x)$ is flat as shown in Fig. 1. $W_1(x)$ is the standard ratchet potential as shown in Fig. 1.

Detailed balance of each of the chemical reaction implies

$$\frac{\alpha_1}{\alpha_2}=e^{(W_1-W_2+\Delta\mu)/k_BT}, \tag{7}$$

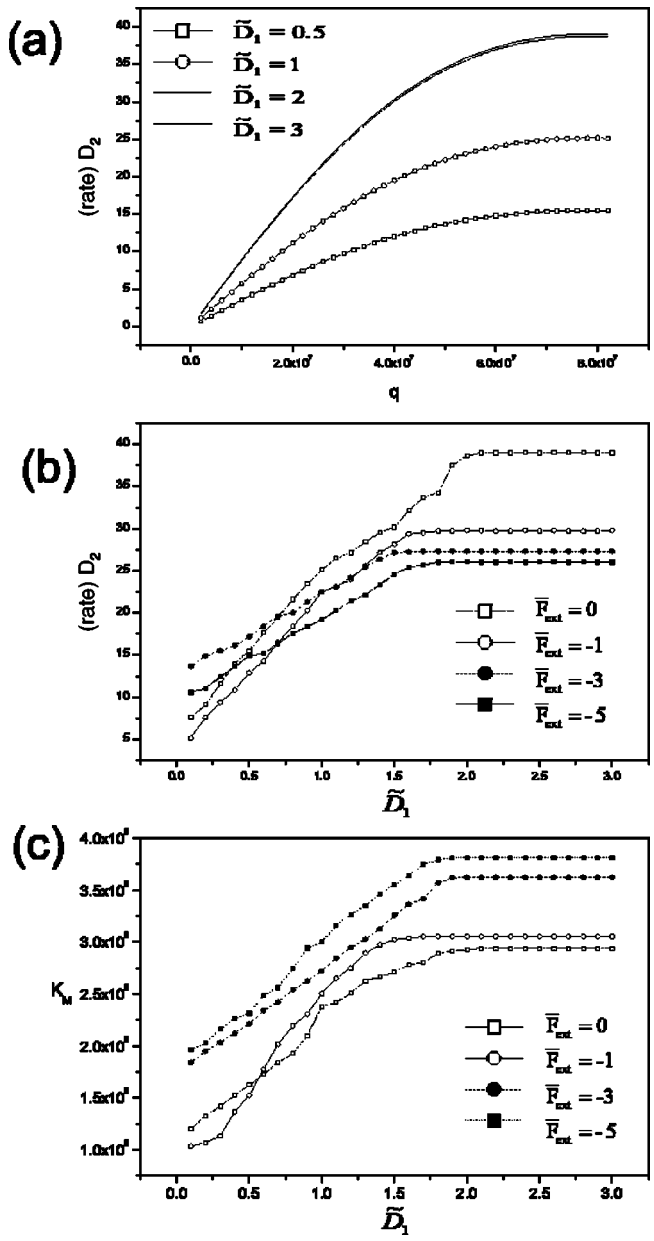


FIG. 2. Simulation results for model A. (a) Rate of ATP consumption as a function of $q=e^{\Delta\mu/k_BT}$. (b) The maximum rate $r_{\max}$ for $F_{\text{ext}}=0,-1,-3,-5$. (c) Michaelis-Menten constant $K_M$ for $F_{\text{ext}}=0,-1,-3,-5$.

$$\frac{\beta_1}{\beta_2}=e^{(W_1-W_2)/k_BT}, \tag{8}$$

where the chemical driving force

$$\Delta\mu\equiv\mu_{ATP}-\mu_{ADP}-\mu_P. \tag{9}$$

Then the transition rates in the Fokker-Planck equation become

$$\omega_1(x)=\alpha_1(x)+\beta_1(x),\omega_2(x)=\alpha_2(x)+\beta_2(x). \tag{10}$$

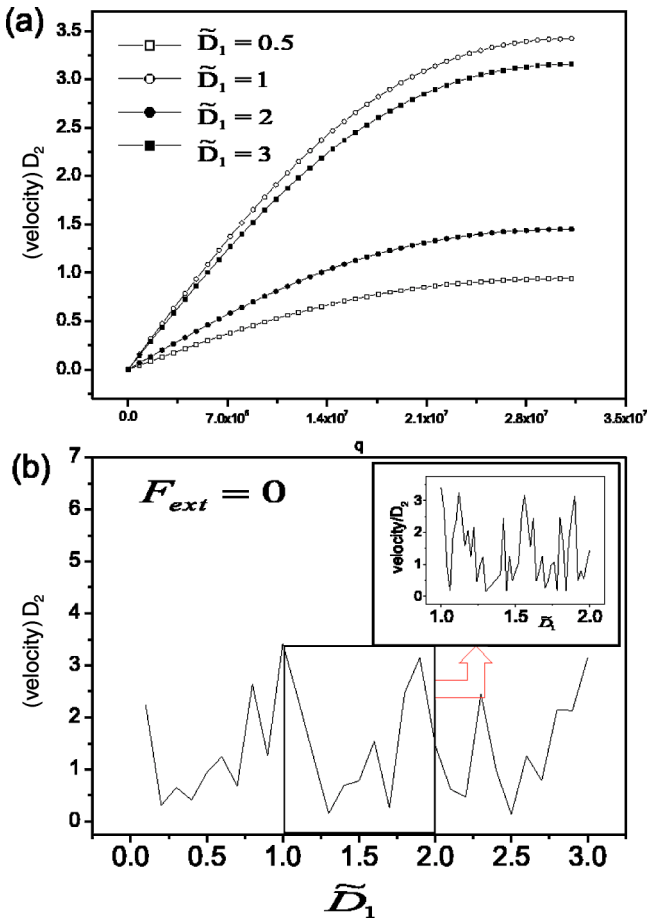


FIG. 3. (a) Velocity curves as a function of $q=e^{\Delta\mu/k_BT}$ for model *A* when $F_{\text{ext}}=0$. (b) Maximum velocity as a function of $\tilde{D}_1$ for $0<\tilde{D}_1<3$ with $\Delta\tilde{D}_1=0.1$. Shown in the inset is the velocity curve measured with $\Delta\tilde{D}_1=0.02$

If we maintain the constant external load, we can look for a stationary solution. Then the average velocity and the rate of ATP consumption become

$$v=\int_0^L [J_1(x)+J_2(x)]dx, \tag{11}$$

$$r=\int_0^L [\alpha_1 P_1-\alpha_2 P_2]dx. \tag{12}$$

As a result of the broken detailed balance ($\Delta\mu\neq 0$) and asymmetry of the potential, the motor can acquire nonzero average velocity and can work mechanically against a load.

In the presence of an external force $F_{\text{ext}}$, the system can perform mechanical work. The work performed per unit time against the external force is

$$\mathcal{W}=-F_{\text{ext}}v. \tag{13}$$

The chemical energy consumed per unit time is given by

$$\mathcal{Q}=r\Delta\mu. \tag{14}$$

We can now define the efficiency of energy transduction

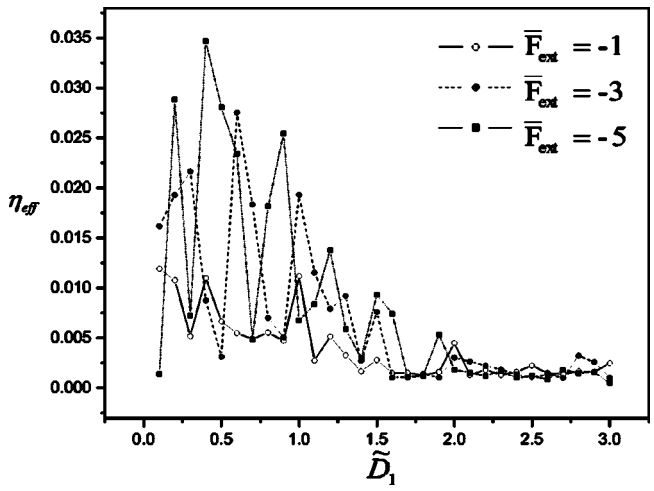


FIG. 4. Efficiency of model *A* as a function of $\tilde{D}_1$ for $F_{\text{ext}}=-1,-3,-5$.

$$\eta=-\frac{F_{\text{ext}}v}{r\Delta\mu}. \tag{15}$$

Since the release of products is just a thermal transition, we assume that $\beta_2(x)=\omega=\text{const}$ as in Ref. [15]. It is known that chemical reactions such as the ATP-binding step are restricted to occur within an active site of conformation space corresponding to the potential minimum [10]. To take into account this concept of active site, we define

$$\alpha_2(x)\sim\begin{cases}\omega & \text{for } L(1-\delta)<x<L\\ 0 & \text{otherwise.}\end{cases} \tag{16}$$

We studied the case in which $\delta=0.05$, 0.3, 1. We call the corresponding models as model *A*, *B*, and *C*, respectively.

## III. SIMULATION RESULTS

We now rescale the above equations into a dimensionless form by setting $\bar{x}=x/L$, $\bar{t}=t/(L^2/D_2)$, $\bar{W}_i\rightarrow W_i/k_BT$, $\bar{F}_{\text{ext}}$

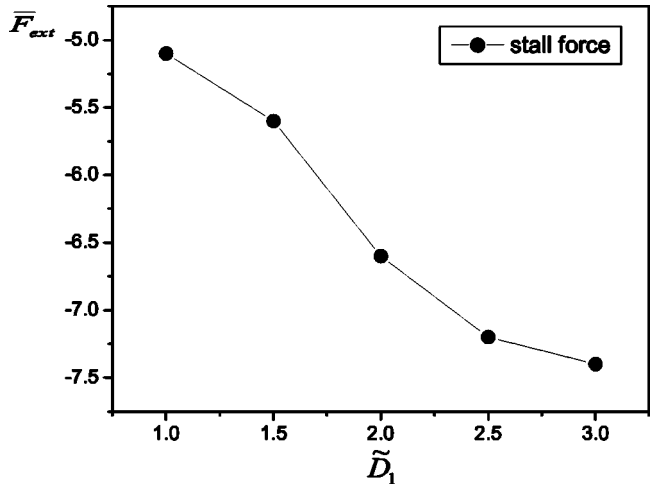


FIG. 5. Stall force for model *A* increases with $\tilde{D}_1$.

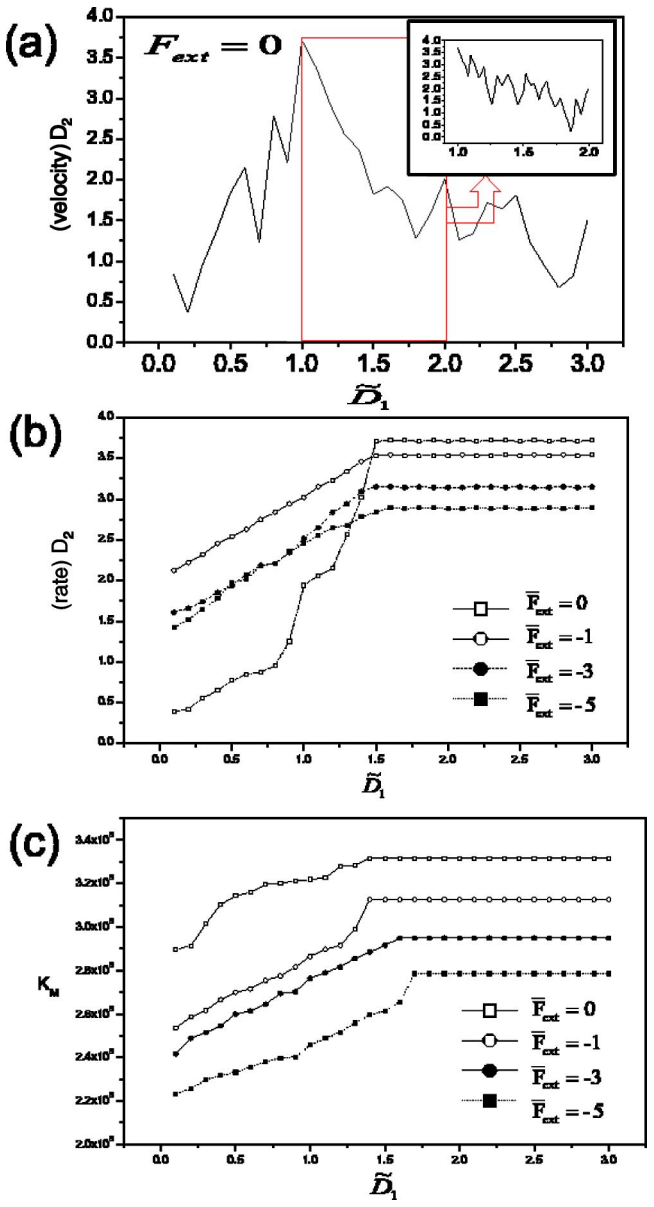


FIG. 6. (a) Maximum velocity of model *B* as a function of $\tilde{D}_1$ for $0<\tilde{D}_1<3$ with $\Delta\tilde{D}_1=0.1$. Shown in the inset is the velocity curve measured with $\Delta\tilde{D}_1=0.02$. (b) Rate curves for model *B*. (c) Michaelis-Menten constant $K_M$ for model *B* when $\bar{F}_{\rm ext}=0,-1,-3,-5$.

$=F_{\rm ext}L/k_BT$, and $\bar{\omega}_i=\omega_i L^2/D_2$. Then the Fokker-Planck equations for a rescaled probability $\bar{P}_i(\bar{x})=LP_i(x)$ become

$$\frac{\partial \bar{P}_1}{\partial \bar{t}} - \tilde{D}_1 \partial_{\bar{x}}[\bar{P}_1(\bar{x},\bar{t})\partial_{\bar{x}}\bar{W}_i - \bar{P}_1(\bar{x},\bar{t})\bar{F}_{\rm ext} + \partial_{\bar{x}}\bar{P}_1(\bar{x},\bar{t})] = -\bar{\omega}_1(\bar{x})\bar{P}_1 + \bar{\omega}_2(\bar{x})\bar{P}_2, \tag{17}$$

$$\frac{\partial \bar{P}_2}{\partial \bar{t}} - \partial_{\bar{x}}[\bar{P}_2(\bar{x},\bar{t})\partial_{\bar{x}}\bar{W}_i - \bar{P}_2(\bar{x},\bar{t})\bar{F}_{\rm ext} + \partial_{\bar{x}}\bar{P}_2(\bar{x},\bar{t})] = \bar{\omega}_1(\bar{x})\bar{P}_1 - \bar{\omega}_2(\bar{x})\bar{P}_2, \tag{18}$$

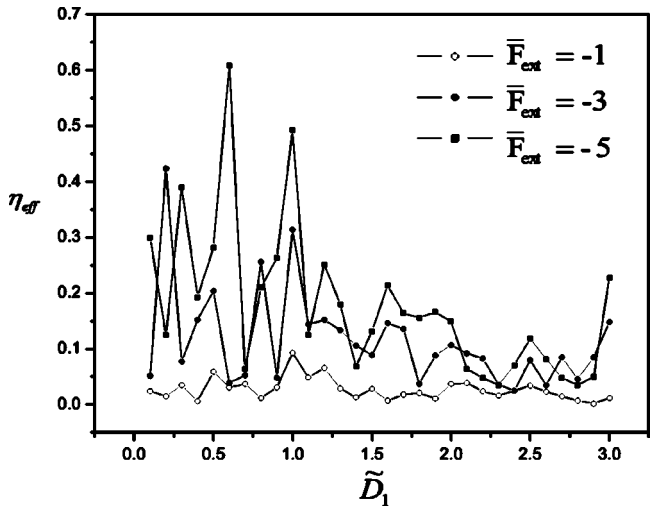


FIG. 7. Efficiency of model *B* as a function of $\tilde{D}_1$ for $\bar{F}_{\rm ext}=-1,-3,-5$.

where $\tilde{D}_1=D_1/D_2$. If we maintain constant external force, the system goes to a steady state with $\partial t P_i=0$. We have obtained the steady state solutions of Eqs. (17) and (18) when we apply an external force $F_{\rm ext}$ and chemical driving force $\Delta\mu$ for a given parameter value of $\tilde{D}_1$. We now perform numerical simulations on a one-dimensional lattice, using the forward time centered scheme with ADI operator method [16]. The equations are discretized with $\Delta x=0.001$ and time interval $\Delta\bar{t}=0.000\,001$. We start with an initial random probability density $P_i(x,0)$ and then numerically integrate Eqs. (17) and (18). At a time step of $10^6$, the density goes to a constant value and we get a stationary solution. In our study, we set the transition rate to $\omega L^2/D_2=50$. In model *A*, the active site is localized to the potential minimum such that the ATP assisted transition can only occur for $0.95<\bar{x}<1$. In model *B*, the ATP assisted transition occurs for $0.7<\bar{x}<1$. To fully investigate the localization effect of the active site, we studied model *C*, where $\alpha_2$ in Eq. (16) is

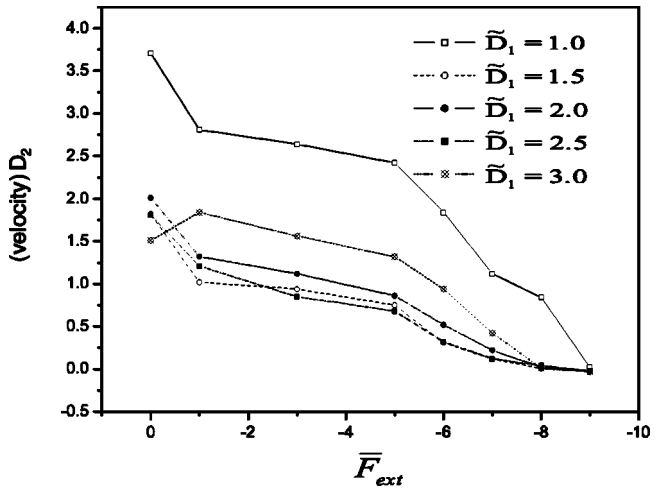


FIG. 8. Force-velocity curve of model *B* as a function of $\bar{F}_{\rm ext}$ when $\tilde{D}_1=1$, 1.5, 2.0, 2.5, and 3.0.

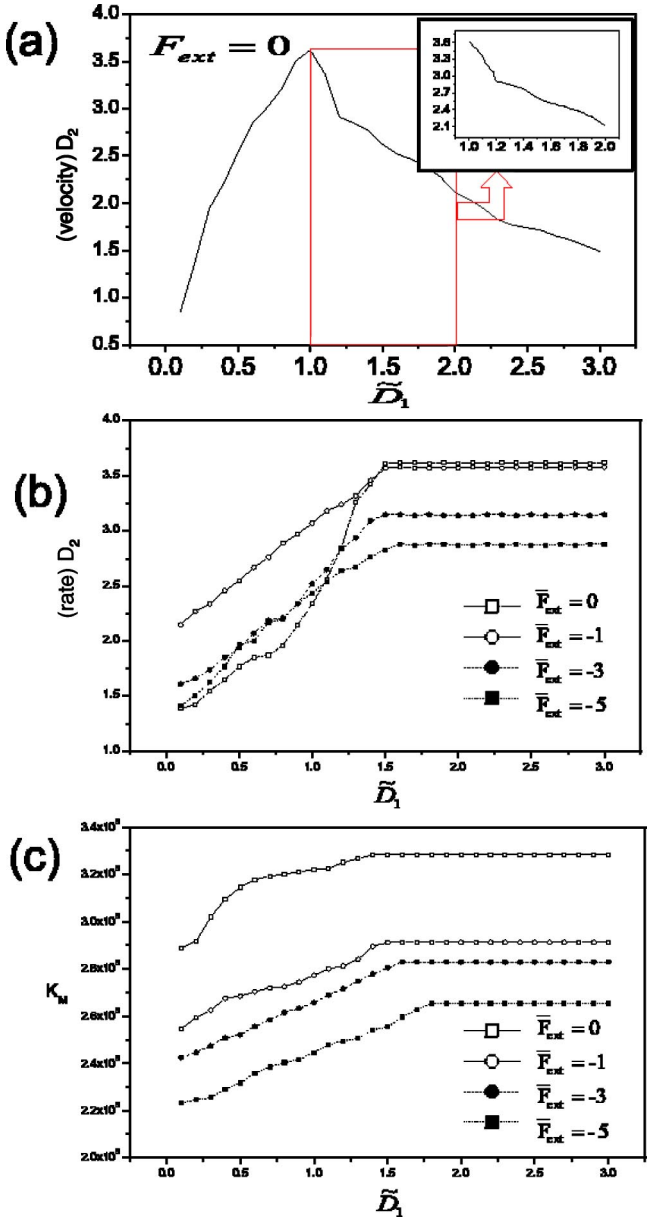


FIG. 9. (a) Maximum velocity of model $C$ when $F_{\text{ext}}=0$ as a function of $\tilde{D}_1$ for $0<\tilde{D}_1<3$ with $\Delta\tilde{D}_1=0.1$. Shown in the inset is the velocity curve measured with $\Delta\tilde{D}_1=0.02$ (b) Simulation results for the ATP consumption rate for model $C$. (c) Michaelis-Menten constant $K_M$ for model $C$ when $\bar{F}_{\text{ext}}=0,-1,-3,-5$.

constant for all $\bar{x}$ ($\delta=1$). Figure 2(a) shows the rate of ATP consumption curves plotted in terms of

$$q=\exp(\Delta\mu/k_BT) \tag{19}$$

for various values of $\tilde{D}_1$. Figure 2(b) shows the value of $r$ at the saturating ATP concentration as a function of $\tilde{D}_1$ for various values of external load.

We find that the rate of ATP consumption can be fitted into the form

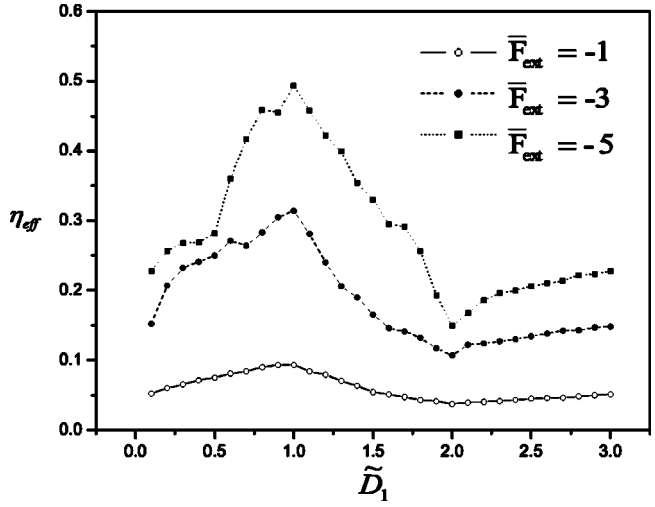


FIG. 10. The efficiency of model $C$ as a function of $\tilde{D}_1$ for $\bar{F}_{\text{ext}}=-1,-3,-5$.

$$r=\frac{r_{\max}q}{K_M+q}, \tag{20}$$

obeying Michaelis-Menten law with $q$ replaced with ATP concentration. Figure 2(c) shows Michaelis-Menten constant $K_M$ obtained from Eq. (20). We find that the value $r_{\max}$ is weakly dependent on the applied force.

Figure 3(a) shows simulation results for the velocity for model $A$ as a function of $q$, which shows that velocity approaches a maximum value at $q\to\infty$

Shown in Fig. 3(b) is the maximum velocity profile for model $A$ at the saturating ATP concentration for $F_{\text{ext}}=0$. We find that the velocity profile changes very sensitively as we change the value of $\tilde{D}_1$ with $\Delta\tilde{D}_1=0.1$, in contrast with the rate curve shown in Fig. 2(b). To further investigate this aspect, we obtained the velocity profile as we changed the value of $\tilde{D}_1$ at a discrete step of $\Delta\tilde{D}_1=0.02$, shown in the inset of Fig. 3(b). We find that the velocity profile depends more sensitively on the value of $\tilde{D}_1$.

If we try to fit the velocity by a Michaelis-Menten equation of the form Eq. (1), we obtain a value of $K_M$, which differs from that obtained though Eq. (20). Furthermore, $K_M$ becomes a very sensitive function of $\tilde{D}_1$, similar to that of the velocity shown in Fig. 3(b). Instead we apply a modified Michaelis-Menten law

$$v=\frac{\alpha r_{\max}q}{K_M+q}-\beta. \tag{21}$$

Then we obtain the same identical value of Michaelis-Menten constant as that obtained from the rate curve shown in Fig. 2(b). Similar to the case of $\tilde{D}_1=1$ [14], positive values of $\beta$ indicate that we have a nonzero ATP consumption even under the stall condition ($v=0$). Figure 4 shows the efficiency curves for the different values of external load calculated from Eq. (15). We find that the efficiency $\eta$ is very low and goes to zero as $\tilde{D}_1$ becomes larger than 2. We note that the stall force increase monotonically with increas-

ing $\tilde{D}_1$ for small $F_{\text{ext}}$, but the increment decreases for a larger value of $F_{\text{ext}}$ (see Fig. 5).

In order to understand the active site effect on the ATP assisted transition, we study model *B*, where $\beta_2$ is nonzero for $0.7<\overline{x}<1$. Figures 6(a), 6(b), and 6(c) show the velocity, the rate, and the Michaelis-Menten constant as a function of $\tilde{D}_1$ for various values of $F_{\text{ext}}$. We find that the Michaelis-Menten constant becomes smaller for a larger external load in contrast to the case of model A. As shown in Fig. 6(b), we note that the maximum velocity also depends sensitively on the value of $\tilde{D}_1$ like the model *A*. The efficiency curve in Fig. 7 shows the efficiency is maximum when $\tilde{D}_1=1$ and increases as we increase the external load. We note that the rate of ATP consumption is smaller and the efficiency becomes larger rather sharply compared with those of model *A*. Figure 8 shows the force-velocity curves for various values of $\tilde{D}_1$. We find that the overall slope of the curve decreases with the increase of $\tilde{D}_1$.

In model *C*, we studied the case in which the ATP assisted transition can occur at all sites with the same rate $\alpha_2=\omega$ ($\delta=1$). Figures 9(a), 9(b), and 9(c) show the velocity, the rate, and the Michaelis-Menten constant as a function of $\tilde{D}_1$ for various values of $F_{\text{ext}}$. We find that Michaelis-Menten constant decreases as we increase the external load similarly to the case of model *B*.

However, the velocity varies rather smoothly as a function of $\tilde{D}_1$ as shown in Fig. 9(a), in contrast to those of model *A* and *B*. The efficiency curve in Fig. 10 clearly shows that efficiency becomes maximum for $\tilde{D}_1=1$. We note that the stall force also increases as we increase $\tilde{D}_1$.

## IV. DISCUSSION

In this paper, we studied a linear molecular motor using a two state ratchet model where diffusion constants of each of two states are different. Our study extends the work done by Lattanzi and Maritan [14], in which the force-velocity relations of a two-state model with identical diffusion constants are studied. In model *A*, where the ATP assisted transition can only occur in a very localized ''active site'' near the minimum of potential between the motor and microtubule, we find that the value of the velocity depends very sensitively on the value of diffusion constants. By providing a modified Michaelis-law, we obtain a unique value of the Michaelis-Menten constant from both the velocity and rate consumption curve, which increases with increasing the external load. Experimental finding [13] that the Michaelis-Menten constant $K_M$ increases with increasing external load seems to indicate that the active site model is an appropriate model to describe biological motor protein.

By studying models where the ATP assisted transition can occur in a wide region such as model *B* and *C*, we find that the Michaelis-Menten constant decreases as the external load increases, contrastingly with the active site model *A*. In ''delocalized'' models, we find that the motor becomes most effective and acquires the maximum velocity when the diffusion constants in both states are same. The efficiency of the model is greatly enhanced in the''delocalized model'' so that it ranges around 30%, which is much larger than that of biological motors.

Through our study, we find that this modified Michaelis-Menten law can be used to explain the velocity curve of a two-state ratchet model with different diffusion constants in each of two states. When the ratio of diffusion constants exceeds 2, the rate of ATP consumption, the velocity of the motor, and the Michaelis-Menten constant become independent of the ratio of diffusion constant. Our study can be used in designing an artificial motor protein.

## ACKNOWLEDGMENTS

This work was supported by the Korea Research Foundation Grant (Grant No. KRF 2001-015-DP0123).

[1] B. Alberts, D. Bray, J. Lewis, M. Raff, K. Roberts, and J.D. Watson, *The Molecular Biology of the Cell* (Garland, New York, 1994).
[2] J. Howard, *Mechanics of Motor Proteins, and the Cytoskeleton* (Sinauer, Sunderland, MA, 2001).
[3] A. Adjari and J. Prost, C. R. Acad. Sci. Ser. II: Mec., Phys., Chim., Sci. Terre Univers **315**, 1635 (1992).
[4] M.O. Magnasco, Phys. Rev. Lett. **71**, 1477 (1994).
[5] J. Prost, J.F. Chauwin, L. Peliti, and A. Ajdari, Phys. Rev. Lett. **72**, 2652 (1994).
[6] C.R. Doering, W. Horsthemke, and J. Riordan, Phys. Rev. Lett. **72**, 2984 (1994).
[7] F. Jülicher and J. Prost, Phys. Rev. Lett. **75**, 2618 (1995).
[8] I. Derényi and T. Vicsek, Phys. Rev. Lett. **75**, 374 (1995).
[9] R.D. Astumian, Science **276**, 917 (1997).
[10] F. Jülicher, A. Adjari, and J. Prost, Rev. Mod. Phys. **69**, 1269 (1997).
[11] T. Duke and S. Leibler, Biophys. J. **71**, 1235 (1996).
[12] J. Howard, A.J. Hudspeth, and R.D. Vale, Nature (London) **342**, 154 (1989).
[13] K. Visscher, M.J. Schnitzer, and S.M. Block, Nature (London) **400**, 184 (1999).
[14] G. Lattanzi and A. Maritan, Phys. Rev. Lett. **86**, 1134 (2001).
[15] A. Parmeggiani, F. Jülicher, A. Ajdari, and J. Prost, Phys. Rev. E **60**, 2127 (1999).
[16] W.H. Press, S.A. Teukolsky, W.T. Vetterling, and B.P. Flannery, *Numericl Recipes in C* (Cambridge University Press, Cambridge, 1986).